Mahdi O. Karkush
Deepankar Choudhury *Editors*

Geotechnical Engineering and Sustainable Construction

Sustainable Geotechnical Engineering

Springer

Geotechnical Engineering and Sustainable Construction

Mahdi O. Karkush · Deepankar Choudhury
Editors

Geotechnical Engineering and Sustainable Construction

Sustainable Geotechnical Engineering

Springer

Editors
Mahdi O. Karkush
Department of Civil Engineering
University of Baghdad
Baghdad, Iraq

Deepankar Choudhury
Department of Civil Engineering
Indian Institute of Technology Bombay
Mumbai, Maharashtra, India

ISBN 978-981-16-6276-8 ISBN 978-981-16-6277-5 (eBook)
https://doi.org/10.1007/978-981-16-6277-5

This Springer imprint is published by the registered company Springer Nature Singapore Pte Ltd.
The registered company address is: 152 Beach Road, #21-01/04 Gateway East, Singapore 189721, Singapore

Contents

Challenges in Foundation Engineering

Development in Geotechnical Engineering

Improving the Gypseous Soil Bearing Capacity Using Geotextile Reinforcement Under Dry Condition

Makki K. Mohsen, Qasim A. Al-Obaidi, and Ayad O. Asker

Abstract Gypseous soil is one of the problematic soils and greatly affects the stability of the engineering structures, especially in Iraq. The main geotechnical problem of this soil is the significant reduction of its bearing capacity upon loading and/or wetting processes due to the dissolution of gypseous cementing bonds. This study aims to improve the soil's bearing capacity by using geosynthetics material in single, double, and triple distribution patterns. The gypseous soil samples were brought from a site near Sawa Lake by coordinates (31°18′42.83″ N, 45°00′49.36″ E) in Al-Muthanna Governorate with gypsum content of 37.35% forms about 3.0 m high under the ground surface. The Soil-Model apparatus of dimensions (60 × 60 × 50) cm is used, while the proposed square footing dimensions are (10 × 10) cm. The main test program investigates the bearing capacity before and after the soil reinforcement with the geotextile layers. The results showed a considerable increase in bearing capacity and the increase of volume change when using the triple phase pattern with the allowable bearing capacity increase for reinforced gypseous soil, especially with the increasing reinforcement layers at the triple reinforcement pattern. The depth of the geotextile layer with the soil mass has a significant effect on the magnitude of the bearing capacity and decreases the settlement. The improvement proportion of soil bearing capacity using Geotextile Reinforcement at dry state is ranged 20–90% for relative densities 30 and 60% and different reinforcement patterns.

Keywords Gypseous soil · Collapse · Improvement · Bearing capacity · Geotextile

M. K. Mohsen · Q. A. Al-Obaidi (✉) · A. O. Asker
Civil Engineering Department, University of Technology, Baghdad, Iraq
e-mail: Qasim.A.Jassim@uotechnology.edu.iq

M. K. Mohsen
e-mail: 40139@uotechnology.edu.iq

A. O. Asker
e-mail: bce.19.60@grad.uotechnology.edu.iq

M. O. Karkush and D. Choudhury (eds.), *Geotechnical Engineering and Sustainable Construction*, https://doi.org/10.1007/978-981-16-6277-5_1

1 Introduction

Collapsible soil is known as any unsaturated soil that passes into a radical changing of particles positions related to loss of volume upon wetting with or without extra load [1, 2]. Gypseous soils cover numerous districts in the world, particularly in parched and semi-arid locales, where the yearly amount of water is inadequate for filtering the gypsum from these soils [3]. Gypseous soil presents a wide collapse potential as a result of its metastable structure. It has weakly dry and damp content in its normal state due to the existence of cementation bonds and an open gypsum structure, especially at unsaturated states or in bone-dry or semi-arid districts. Additionally, change in volume, quick settlement, and a high lowering within the void proportion of a metastable soil structure can happen. Huge volume changes and sudden collapses occur when the soil is immersed in the water beneath steady vertical pressure. Soil distortion happens as a result of the disintegration of the cemented gypsum bonds causes an articulated increment within the compressibility of the soil [4]. The chemical composition of the gypseous soil is ($CaSO_4.2H_2O$). According to Barzanji [5], the soil is considered as slightly gypseous soil if the gypsum amount (3–10%) and highly gypseous soil if the gypsum amount is (25–50%). The collapse potential (CP) of gypseous soil can be estimated in the lab from single or double Oedometer tests where the soil considers as trouble or severe trouble when the collapse potential (CP) exceeds the value of 5% [4, 6, 7]. Geotextiles are considered to have the bearing capacity or have high tensile strength, while soils, in general, are considered low-stress materials and have high compressive strength. Therefore, geotextiles are the ideal material for improving and increasing the efficiency of the soil and thus increasing structural stability. To protect the soil from collapse [8, 9].

2 Material, Equipment, and Test Setup

Soil. The undisturbed soil sample is brought from a site near Sawa Lake, Al-Muthanna Governorate, from a depth of (3.0) m. This region is considered an arid area, and the soil can be defined as the medium to dense light brown silty SAND with white traces of gypsum particles. The soil classification is (SP-SM) according to the Unified Soil Classification System (USCS). The physical and chemical properties of the soil are shown in Table 1.

Geotextile Material. Geotextile soil fabrics or knitting warp is considered one of the successful practical solutions to some problems arising from the nature of the soil. Geotextile is used in road, and railway soil steady on waterways and beach corrosion control, asphalt pavement overlap crack relief, subsurface drainage systems, waterproofing membrane defend on, landfill, landscaping, etc. Its multiple-use functions include Separation, Filtration, Reinforcement and stabilization function, and drainage [8, 9]. The geotextile reinforcement used in this study is displayed in Fig. 1 and Table 2.

Table 1 Physical and Chemical properties of the soil sample

Property	Value	Standard
Physical properties		
Initial water content (%)	6.1	ASTM D 2216
Liquid, plastic and plasticity index (%)	38, 33, 5	ASTM D 4318
Passing sieve No.200 (%)	9.2	ASTM D 422
D10 (mm)	0.08	ASTM D 422
D30 (mm)	0.115	ASTM D 422
D60 (mm)	0.31	ASTM D 422
Cu	3.87	ASTM D 422
Cc	0.53	ASTM D 422
Specific gravity (Gs)	2.37	ASTM D 854
Max. dry density (g/cm^3)	1.62	ASTM D 4253
Opt. moisture content (%)	13.5	ASTM D 4254
Cohesion (kPa)		
For RD = 30%	4	ASTM D3080
For RD = 60%	5.3	
Angle of friction (°)		
For RD = 30%	28.5	For RD = 60%
For RD = 60%	30	
Chemical properties		
Gypsum content (%)	37.3	
Total sulphate content (SO_3) (%)	17.8	
Total soluble salts (TSS) (%)	12.4	

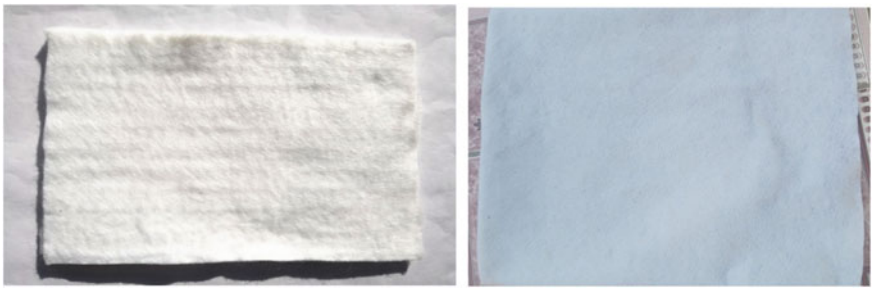

Fig. 1 Geotextile reinforcement was used in this study

Table 2 Geotextile properties

Property	Value	Standard	Property	Value	Standard
Type of geotextile	Nonwoven		Grab tensile strength	750 N	ASTM D4632
Type of fiber	Polypropylene		Wide width tensile strength	13 kN/m	ASTM D4595
Trade name	Prime geo 200		Puncture strength (CBR)	2200 N	ASTM D6241
Weight	200 gm/m^2	ASTM D 5261	Trapezoidal tear strength	280 N	ASTM D4533
Pore size	80 microns	ASTM D 4751	Permittivity	1.6 S^{-1}	ASTM D4491

Soil-Model Apparatus. The Soil-Model Apparatus is made from rigid steel with inner dimensions of the model box are (60 × 60 × 50) cm length, width, and height, the plate thickness of 0.5 cm with square footing (10 × 10 × 1 cm) of rigid steel. The Soil-Model Apparatus consists of several mechanical and electronic parts: Steel load frame, Axial loading system, hydraulic jack, Load cell, a data logger (Adriano), dial gauges, computer software plate, as explained in Figs. 2 and 3.

Sample Preparation. The soil samples are prepared in a test box with a relative density of (30% and 60%). In order to achieve the required dry density, the box is distributed into layers with 50 mm height for every layer and an area of (60 × 60) cm till the full height of 50 cm is reached. The whole number of layers is 10

Fig. 2 Soil-model apparatus during test

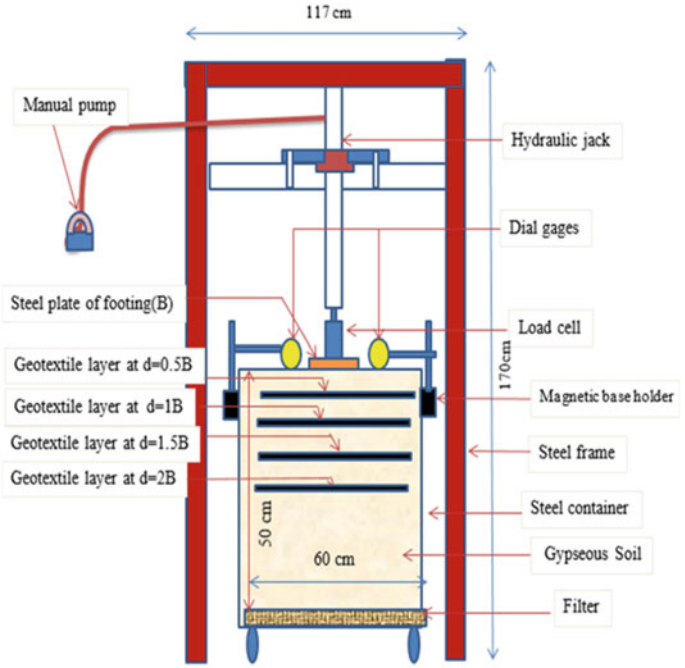

Fig. 3 Diagram of loading system

layers, and the weight of the sandy soil for every layer was (23.11 and 25.36) kg for relative densities 30 and 60%, respectively. Every layer is a store with a level plane and leveled from at that point utilizing the manual compactor instrument until the required density is gotten for all layers as appeared in Fig. 2.

Test Procedure. The compression (i.e., bearing capacity) test is showed by following method nonrepetitive static plate load technique according to the test process mentioned in ASTM D1194-94. The bearing capacity is measured for several layers of geotextile reinforcement with dry conditions of the gypseous soil model. In every case of test, the gypseous soil was put in layers with 5 cm depth. The raining technique measured the position of density. The gypseous soil was placed guardedly on two opposite sides to guarantee a matching density. After setting the final layer, leveled the surface carefully within the straight edge. At that point, the foundation was settled within the center of the test box in x and y trends in unpredictable loading, and after that, the two attractive holders utilizing dial gages within the edge of the box were associated. By the hydraulic jack starts applied the load constantly. The applied load was got from the load cell while the dial gauges determined the settlement. The application of load continuously until to reach the failure. The failure was exposed by the rise of settlement at a constant value of load amount. The diagram of the test setup is shown in Fig. 3.

3 Results and Discussion

To analyze and discuss the effect of using geotextile reinforcement in the gypseous soil under the footing, 20 model tests were carried out consisting of different patterns at the dry state of the soil. For the model tests, the soil bed was prepared with a dry unit weight of 12.84 and 14.1 kN/m^3 identical to a relative density of 30 and 60%, respectively. The bearing capacity tests are divided into two main groups: untreated and treated soil tests. The treated and treated soil tests involve three different categories of soil sample conditions as follows: (10) model tests using a single geotextile layer, (6) model tests using double geotextile layers, and (4) model tests using triple geotextile layers.

Load-Settlement Results. These results display that the performance of load–settlement relations sound to be like the general shear failure relation and refer to the soil failure. The reinforcement geotextile layers were placed at a different depth such as (0.5 B, 1B, 1.5B, and 2B) when B represented the width of footing for all model tests. The results are shown in Figs. 4 and 5 with a relative density of 30 and 60%.

Ultimate Bearing Capacity of Dry Gypseous Soil at Relative Density (30%). Figures 6 explains the experimental work to determine the value of ultimate bearing capacity [untreated] at relative density (30%) by two tangent intersection methods under the square footing.

Ultimate Bearing Capacity of Dry Gypseous Soil at Relative Density (60%). Figures 7 explains the experimental results for determining the values of ultimate bearing capacity [untreated] at relative density (30%) by two Tangent Intersection Method under the square footing.

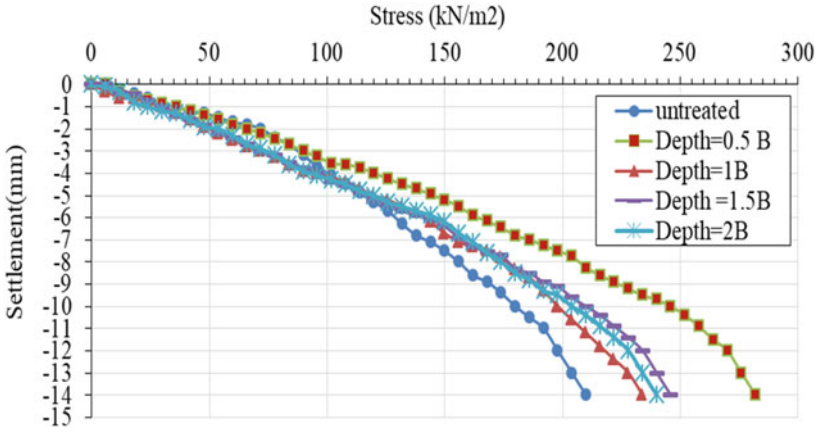

Fig. 4 The relation between the stress and the settlement for gypseous soil in a dry state (reinforced) experimental model (single layer) at RD = 30%

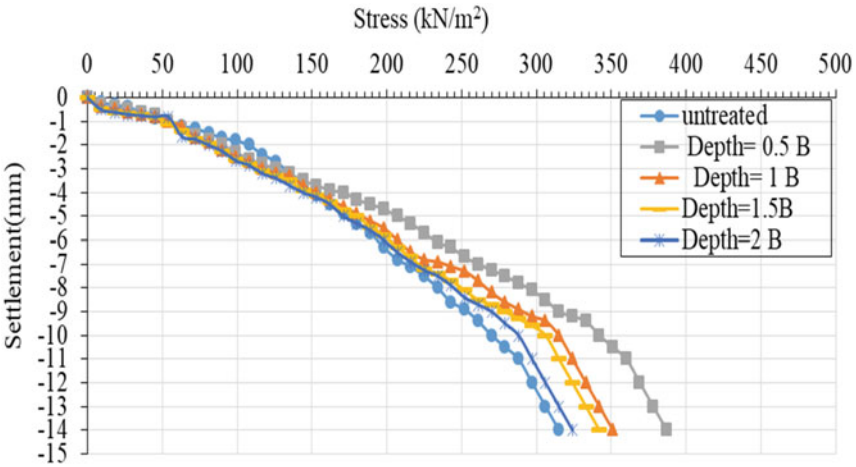

Fig. 5 The relation between the stress and the settlement for gypseous soil in a dry state (reinforced) experimental model (single layer) at RD = 60%

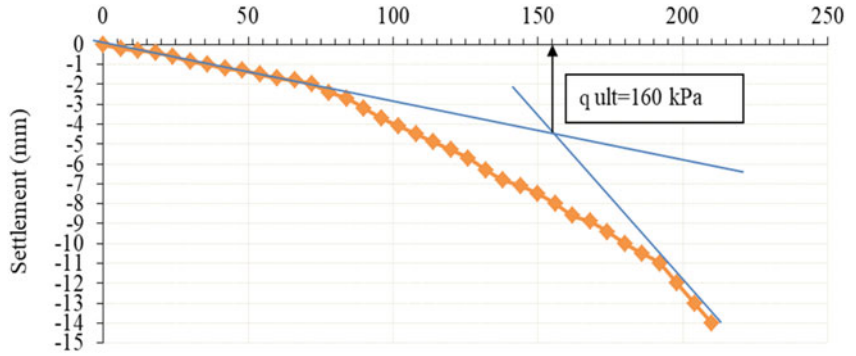

Fig. 6 The relation between the stress and the settlement for gypseous soil in dry State experimental model Result at RD = 30% (untreated)

Comparison of Allowable Bearing Capacity and Relative Density 30 and 60% for Dry Gypseous Soil. Figure 8 explains the relation between allowable bearing capacity and relative density for dry gypseous soil using single-layer geotextile reinforcement. Figure 9 explains the relationship between allowable bearing capacity and relative density for dry gypseous soil when using double-layer geotextile reinforcement. Figure 10 explains the relation between allowable bearing capacity and relative density for dry gypseous soil using triple-layer geotextile reinforcement.

Tables 3 shows the results of experimental work and explains the improvement of using geotextile reinforcement on the bearing capacity of gypseous soil. The geotextile has proved it's effective in improving the bearing capacity and lowering the settlement values, see Figs. 4 and 5. Figures 8, 9 and 10 show a comparison of

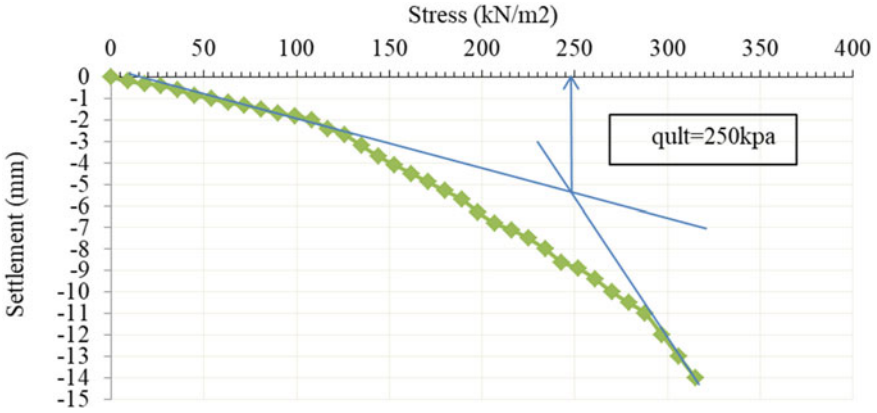

Fig. 7 The relation between the stress and the settlement for gypseous soil in dry State experimental model Result at RD 60% [untreated]

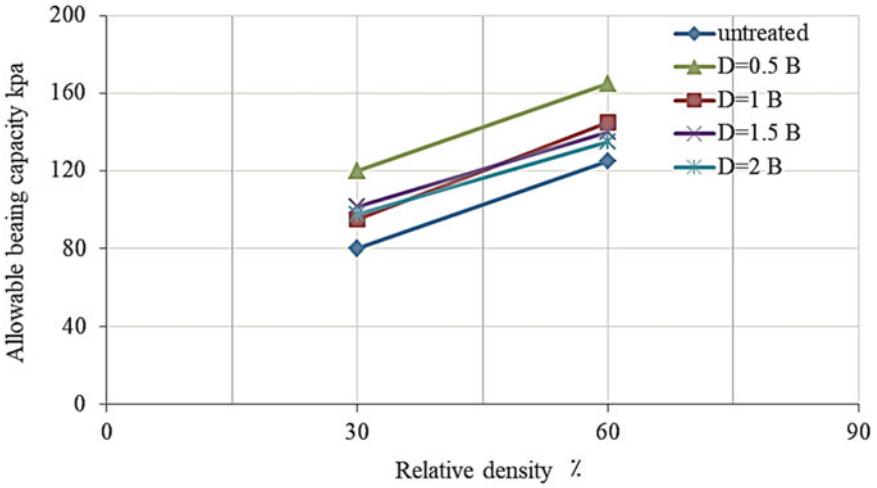

Fig. 8 Allowable bearing capacity and relative density at 30 and 60% relationship (when the dry gypseous soil model samples is treated by single layer of geotextile reinforcement)

allowable bearing capacity and relative density 30 and 60% for dry gypseous soil, the triple-layer phase pattern of geotextile reinforcement at depth (0.5B + 1B + 1.5B) gives a higher value of allowable bearing capacity equal to 155 kPa at RD (30) while equal to 245 kPa at RD (60).

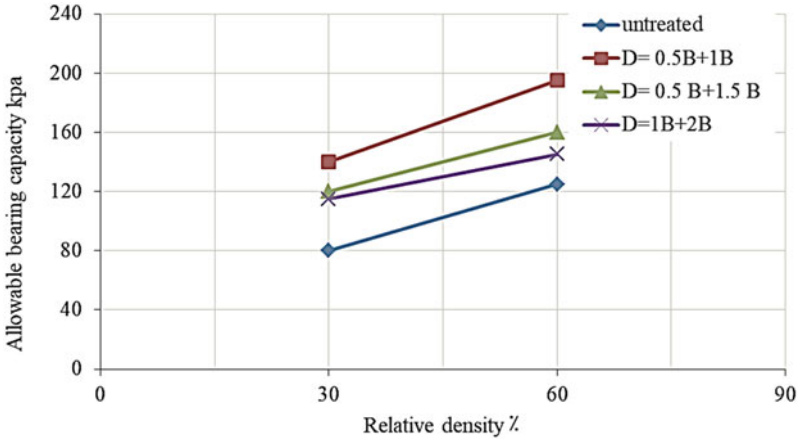

Fig. 9 Allowable bearing capacity and relative density at 30 and 60% relationship (when a double layer treats the dry gypseous soil model samples of geotextile reinforcement)

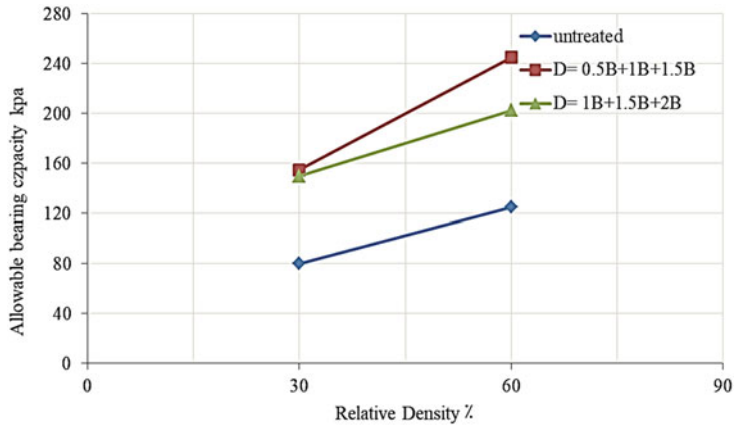

Fig. 10 Allowable bearing capacity and relative density at 30 and 60% relationship (when a triple layer treats the dry gypseous soil model samples of geotextile reinforcement)

4 Conclusions

The following points can be concluded from the results of this study:

- The allowable bearing capacity of gypseous soil increase with the increase of relative density and reinforcement layers, where the allowable bearing capacity was 80 and 125 kPa at relative density 30 and 60%, respectively.

Table 3 The values of ultimate bearing capacity for dry gypseous soil models by two tangent intersection method under square footing in the dry state at RD = 30% and 60%

Test no	Pattern	Depth of placement	RD = 30%		RD = 60%	
			q_{ult} (kN/m^2)	q_{all} (kN/m^2)	q_{ult} (kN/m^2)	q_{all} (kN/m^2)
1	Untreated	–	160	80	250	125
2	Single layer geotextile reinforcement	D = 0.5B	240	120	330	165
3		D = 1B	190	95	290	145
4		D = 1.5B	203	101.5	280	140
5		D = 2B	195	97.5	270	135
6	Double layer geotextile reinforcement	D = 0.5B + 1B	280	140	390	195
7		D = 0.5B + 1.5B	240	120	320	160
8		D = 1B + 2B	230	115	290	145
9	Triple layer geotextile reinforcement	D = 0.5B + 1B + 1.5B	310	155	490	245
10		D = 1B + 1.5B + 2B	300	150	405	202.5

- The reinforcement pattern, depth (i.e., position), and a number of the reinforcement geotextile layer have a large effect on the allowable bearing capacity of gypseous soil.
- For a single geotextile layer model, the maximum value of allowable bearing capacity when the reinforcement is at depth (0.5B) with q_{all} was 165 kPa at relative density 60%, while the minimum value of allowable bearing capacity when the reinforcement is at depth (1 B) with q_{all} was 95 kPa at relative density 30%.
- For the double geotextile layer model, the maximum value of allowable bearing capacity when the reinforcement is at depth (0.5 B + 1 B) with q_{all} was 195 kPa at relative density 60%, while the minimum value of allowable bearing capacity when the reinforcement is at depth (1B + 2B) with q_{all} was 115 kPa at relative density 30%.
- For the triple geotextile layer model, the maximum value of allowable bearing capacity when the reinforcement is at depth (0.5 B + 1 B + 1.5 B) with q_{all} was 245 kPa at relative density 60% while the minimum value of allowable bearing capacity when the reinforcement is at depth (1 B + 2 B) with q_{all} was 150 kPa at relative density 30%.

References

1. Ahmad, F., Said, M. A., & Najah, L. (2012). Effect of leaching and gypsum content on properties of gypseous soil. *International Journal of Scientific and Research Publications, 2*(9), 1–5.
2. Al-Obaidi, Q. A., Ibrahim, S. F., & Schanz, T. (2013). Evaluation of collapse potential investigated from different collapsible soils. In *Multiphysical testing of soils and shales* (pp. 117–122) Berlin, Heidelberg: Springer.
3. Fattah, M. Y., Obead, I. H., & Omran, H. A. (2019). A study on leaching of collapsible gypseous soils. *International Journal of Geotechnical Engineering*, 1–11.
4. Al-Obaidi, Q. A., Karim, H. H., & Al-Shamoosi, A. A. (2020, February). Collapsibility of gypseous soil under suction control. In *IOP Conference Series: Materials Science and Engineering* (Vol. 737, No. 1, p. 012103). IOP Publishing.
5. Jha, A. K., & Sivapullaiah, P. V. (2017). Unpredictable behaviour of gypseous/gypsiferous soil: An overview. *Indian Geotechnical Journal, 47*(4), 503–520.
6. Al-Saoudi, N. K., Al-Khafaji, A. N., & Al-Mosawi, M. J. (2013). Challenging problems of gypseous soils in Iraq. In *Proceedings of the 18th International Conference on Soil Mechanics and Geotechnical Engineering* (pp. 479–482).
7. Fattah, M. Y., Joni, H. H., & Al-Dulaimy, A. S. (2016). Compaction and collapse characteristics of dune sand stabilized with lime-silica fume mix. *Earth Sciences Research Journal, 20*(2), 1–8.
8. Koerner, R. M. (2005). *Designing with geosynthetic.* 5th edn. (P. 796) USA: Pearson Prentice Hall.
9. Tawfeeq, S. S. (2009). *Performance of geosynthetics to improve gypseous soils.* Thesis, Civil Engineering Department, University of Tikrit, Iraq.

Numerical Modeling of Circular Tunnel Alignment Under Seismic Loading

Hayder A. Al-Mirza and Mahdi O. Karkush

Abstract The continuous increase in population has led to the development of underground structures like tunnels to be of great importance due to several reasons. One of these reasons is that tunnels do not affect the living activities on the surface, nor they interfere with the existing traffic network. More importantly, they have a less environmental impact than conventional highways and railways. This paper focuses on using numerical analysis of circular tunnels in terms of their behavior during construction and the deformations that may occur due to overburden and seismic loads imposed on them. In this study, the input data are taken from an existing Cairo metro case study; results were found for the lateral and vertical displacements, the Peak Ground Acceleration (PGA), Arias Intensity (I_A), and the Fourier amplitude spectrum. It was found that the vertical displacement was 26.2 mm under overburden pressure and reached 28 mm under seismic loading. These results were discussed and compared to other information and given a logical explanation based on the findings.

Keywords Tunnels · Alignment · Seismic loading · Numerical modeling · PLAXIS 3D

1 Introduction

In the middle and southern parts of Iraq, natural soil characteristics from an engineering perspective are inadequate and require additional precautions when building a superstructure or an underground structure. Recently, Baghdad has witnessed some earthquakes, so with this problem comes the necessity to do thorough studies regarding soil behavior in such conditions. The reason for that is because, in the future, one should be prepared for worst-case scenarios when designing an underground structure in such relatively weak soils. On the other hand, transportation

H. A. Al-Mirza (✉) · M. O. Karkush
Department of Civil Engineering, University of Baghdad, Baghdad, Iraq
e-mail: h.almirza1901m@coeng.uobaghdad.edu.iq

M. O. Karkush
e-mail: mahdi_karkush@coeng.uobaghdad.edu.iq

M. O. Karkush and D. Choudhury (eds.), *Geotechnical Engineering and Sustainable Construction*, https://doi.org/10.1007/978-981-16-6277-5_2

infrastructures like highways, railways, and tunnels used for sanitation purposes have become a challenging topic over the years due to advancements in this field. In recent decades, there have been numerous studies on tunnels under seismic loadings, and it became more accessible with the development of software that evaluates the load-deformation of tunnels along with other parameters. Tunnels' resistance to static and seismic damage is generally dependent on a variety of factors: the overburden and seismic response of surrounding ground. In order to ensure the safety and serviceability of the underground structure, detailed design and construction procedures have to be carried out, taking into account all possible outcomes.

Although tunnels are considered a crucial part of the transportation infrastructure today, there are many problems related to the tunneling process, whether about the construction itself and its effect on the surrounding buildings or the post-construction long-term impact on tunnel parts. Most studies have showed interest in this topic whether regarding the tunnel face stability [1] or the behavior of a tunnel under deformation [2]. On the other hand, a case study of the Cairo Metro used PLAXIS 3D numerical analysis, which assumed a hardening soil model and evaluated the lateral and vertical displacements under static loading [3]. Also, a database has been created for earthquakes worldwide, documenting the effect on different tunnels and the different levels of damage from which they have suffered. Evidently, the seismic loading can really have a detrimental influence on the tunnel lining, and many factors can contribute to this, such as frequency, amplitude, and magnitude, and this influence is governed by the tunnel length, thickness, and other structural parts. Based on the previous literature, one should simulate a model and study the aforementioned factors numerically so as to evaluate this model under conditions similar to actual cases. The proposed research paper will focus on the response of tunnels under overburden and seismic loading conditions by creating finite element models of a circular tunnel, Cairo tunnel. The variables that will be assessed, as mentioned earlier, include the tunnel face stability during construction and the magnitude of the earthquake, its amplitude and frequency, and their effect on circular tunnels. This paper will consist of the impact of vertical propagation of seismic waves and the overburden loadings on the tunnel. The resulting displacement from these loadings will also be discussed in detail in the following sections.

2 Alignment of Tunneling

According to King and Kuesel [4], the governing factors that determine the tunnel's feasibility and route include the soil's geological conditions, cost, and construction time. The types of tunnels can be classified based on purpose, alignment, and shape. The geometry is different from one tunnel to another based on its purpose as prescribed by the American Association of State Highway and Transportation Officials (AASHTO). A two-lane highway tunnel should be 3.5 m wide each, while the right shoulder should provide a sufficient area for disabled vehicles and the left

one should provide a space for motorists. Additionally, trunk highway tunnel's clearance should be at least 4.5 m with additional vertical clearance for traffic lights and signs, ventilation systems, and lighting. Table 1 shows the relationship between the construction method and the tunnel shape [5].

Tunnel Face Stability. One of the most crucial factors that should be looked into when constructing a tunnel in weak soils is the tunnel face's stability. According to Broere [6], despite the support type used in the process, the boring machine chamber pressure should be kept at a certain level to ensure stable working conditions. This means that the pressure should not be so high that deformation happens in the soil, nor should it be so low that uncontrolled collapse occurs. During the process of validating the failure assumptions, Broere [6] has carried out laboratory tests to distinguish the failure mechanisms in clay and sand, and the finding was so distinct because, in the sand, the failure takes the shape of a chimney while in clay it is much larger and broader.

Time and Cost-Related Problems. One of the main problems related to tunnel construction projects is that they substantially cost more than open highways or railways because these kinds of projects require extensive investigations and design criteria. Paraskevopoulou and Benardos [7] have investigated 258 projects in 20 countries, and they have found that one major problem in these projects is the cost underestimation and that 90% of these projects have exceeded their initial estimation regarding the cost. When it comes to time consumption, these projects during their various stages will consume time because each stage requires additional work due to many uncertainties to achieve the required goal instead of conventional projects.

Tunnel Convergence. Advancing in tunnel excavation will create pressure on the surrounding soil, and this soil will undergo deformation due to this advancement. This phenomenon is called "convergence" and it requires field and numerical analyses to be fully understood.

Squeezing Ground. According to Schubert and Radoncic [8], the term "squeezing ground" refers to the deformation occurring in zones with high overburden pressure, which is generally encountered either during the construction of the tunnel or afterward. Whether the tunnel is constructed in rock or weaker soils, the lining should be allowed for specific strains. Due to the difficulty of predicting the ground conditions,

Table 1 Tunnel type versus construction method

Construction Method	Rectangular	Circular	Horseshoe	Oval
Shield-driven	*	*		
Cut-and-cover	*			
Immersed Tube	*			
Drilling and Blasting			*	*
Sequential Excavation			*	*

it is imperative to adjust the excavation process and support method by using monitoring techniques for the displacement to understand better the mechanical processes happening around the tunnel.

3 Seismic Loading

This field of study is a crucial part of geotechnical engineering and plays an essential role in civil infrastructure nowadays because it involves studying the design for overburden loads and seismic conditions as an additional load. With the increasing population rate, tunnels have become an essential aspect where they are used for transportation means. Until recently, the soil-structure interaction was not considered a significant problem and was not given the needed attention because, in general, the embedded structures have performed well under seismic conditions compared to superstructures. But post-earthquake investigations have shown that tunnels tend to be susceptible during earthquakes or even collapse if seismic design requirements are not met. To better comprehend tunnels stability, one should assess the factors that include peak acceleration and velocity, magnitude and duration of the earthquake, the shape of the tunnel, overburden pressure, and soil type. Underground structures behavior is quite different from that of above-ground structures because the former suffers from kinematic loads of ground rather than the underground structure's inertial loads. As previous earthquakes have proven, tunnels seismic response is highly dependent on the soil-structure interaction (SSI). This leads to the conclusion that the depth, shape, and dimensions of the tunnel, relative stiffness of soil to the tunnel, properties of the ground itself and its seismic response, and the interface, play a significant role in the seismic design of tunnels. Concerning the intensity of earthquakes near Baghdad, Al-Taie and Albusoda [9] investigated the Halabja earthquake case study. They found that some earthquakes have been observed in the last few decades in Baghdad that have caused some damages to structures in the vicinity, as shown in Table 2.

Table 2 Earthquake intensity in Baghdad and the vicinity

Year	Earthquake Richter scale	Observations
1960	Max. 6.7	Caused damages in Halabja and felt in Baghdad
1967	6.1	Observed 100 km south of Halabja
2013	5.1 and 5.8	The two earthquakes were 60 km south of Halabja
2017	7.3	30 km south of Halabja with a maximum earthquake magnitude of 7.3
2018	Max. 4.5	Maximum magnitude was 4.5 in the Northeastern part of Baghdad
2021	4.9	Recorded in Baghdad. (Source: earthquaketrack.com)

4 Numerical Modeling

Because soil-structure interaction representation in an underground structure is somewhat complex and requires a substantial amount of money and time, numerical modeling was always used for this purpose. There are plenty of methods to analyze a tunnel to get the needed relationships, whether regarding the tunnel's deformed shape or the stresses and displacements. These methods include the finite element (FEM), discrete element (DEM), boundary element (BEM), and finite difference method (FDM). FEM is used extensively in engineering applications and can be represented either by using 2-dimensional or 3-dimensional software, and this representation takes the body as elements and analyzes them accordingly. According to Pradhan and Chakraverty [10], it is used for various applications, whether for structural analyses or soil modeling. Hutton [11] defines it as a computational method whose purpose is to find an approximate solution in boundary value problems. To simplify it even further, it allows the continuum to be modeled and separated into a finite number of elements, studies their characteristics, and then assembles these elements to estimate the continuous domain's properties. The implementation of FEM has been developed over the years and is being used rigorously in engineering and applied sciences applications [12]. In this paper, an FE model for the soil and the circular tunnel was created using PLAXIS 3D software, and overburden and seismic loading states were simulated. First, the soil body was defined with 60 m width, 10 m length, and 35 m depth, and a borehole was created in four different layers, each with distinct soil characteristics and depth [3].

It is worth mentioning that the tunnel lining was given properties equivalent to the adjacent soil, and the cohesion for the 4th soil layer was given a value so that the tunnel would not collapse during the tunneling process (see Table 3). The second step was creating the tunnel at a depth of 10 m using the tunnel designer tool in the software with a diameter of 9.4 m, and properties were given for TBM shield as shown in Table 4. The interface between the soil and structure was also created and given a virtual thickness factor of 0.1 for the tunnel lining to assume a case of full-slip boundary conditions in order to consider an infinite domain. After that, the trajectory was defined at 10 m segment length with slices of 1 m each and using the TBM excavation method; four steps were created for tunnel crown and invert excavation process and lining application. Also, the seismic load was applied in the x and z directions with a load multiplier of frequency of 5 Hz as stated in El-Naggar and Bentley [13]. Moreover, a finely distributed element mesh was generated, and the water table was set at 2 m below the surface as assumed by El-Nahhas et al. [3] (see Fig. 1).

Using Python script as the tunnel advancement tool, the tunnel took 12 phases for the excavation and TBM shield installment using TBM sequence, and during this advancement the failure criterion was the soil collapse potential. Moreover, one additional phase was added for applying the seismic load in the x-direction and one phase for the same load in the z-direction. The seismic load was simulated in phases 13 and 14 with 0.5 s dynamic time interval, and the displacement was dependent on

Table 3 Soil properties in HS material model

Parameter	1st layer	2nd layer	3rd layer	4th layer	Unit
Material model	HS	HS	HS	HS	–
Material behavior	Drained	Drained	Drained	Drained	–
Depth	3	1.5	5	25.5	m
Unsaturated unit weight	17	18	19	20	kN/m^3
Saturated unit weight	17	18	19	20	kN/m^3
Cohesion	0	80	0	25	kPa
Internal friction	15	0	30	37	o
Secant triaxial test stiffness	7230	9100	20,310	35,430	kPa
Tangent stiffness	7230	9100	20,310	35,430	kPa
Unreload/reload stiffness	21,680	27,300	60,930	106,290	kPa
Shear modulus at small strain	37,500	59,340	116,210	170,590	kPa
Shear strain at $G_s = 0.722G_o$	1.61E−04	5019E−04	2.79E−04	4.52E−04	–
Power for stress law	0.5	1	0.5	0.5	–
Reference stress	100	100	100	100	kPa
Poisson's ratio	0.2	0.2	0.2	0.2	–
Coefficient of lateral stress	0.74	1	0.5	0.4	–
Failure ratio	0.7	0.75	0.8	0.8	–
Interface strength	Rigid	Rigid	Rigid	Rigid	–

Table 4 TBM shield material properties

Parameter	TBM	Unit
Thickness	0.14	m
Unit weight	70	kN/m^3
Elasticity modulus	26×10^7	kPa
Poisson's ratio	0.3	–
Shear modulus	10^8	kPa

the tunneling process's previous phases. The model used for analysis was Paradiso multicore direct with maximum cores of 256, 1000 maximum number of steps, and 60 maximum number of iterations allowed with 0.01 tolerated error. The results of settlement under the overburden, excavation, and the seismic pressures will be discussed in the next section.

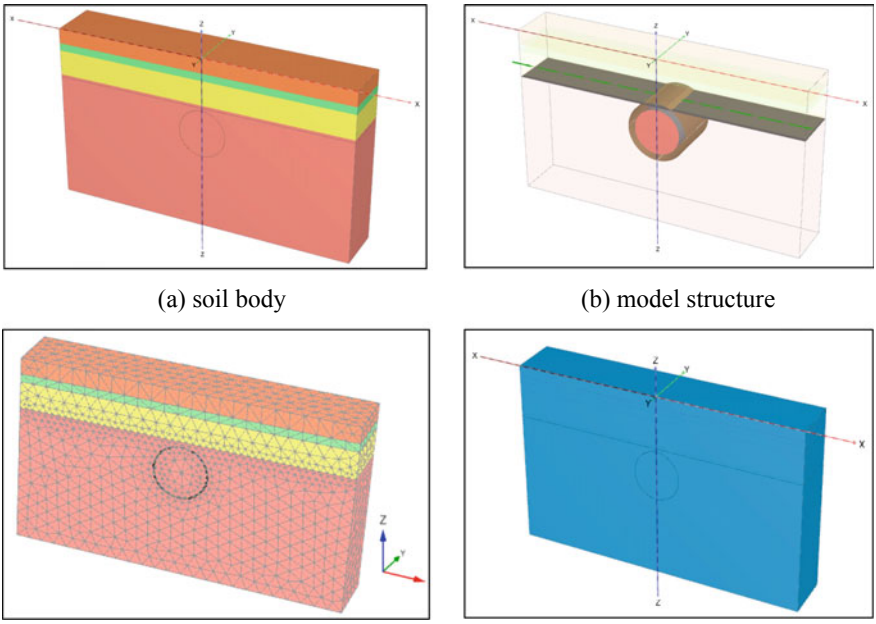

(a) soil body (b) model structure

(c) model mesh (d) global water level

Fig. 1 PLAXIS 3D FE model of the case study

5 Results and Discussion

Starting with Phase 1 to excavate the upper half of the tunnel portal in the first slice, the total displacement was approximately 8.5 mm at the tunnel portal crown. When the lower half of the first slice was excavated the settlement almost doubled and reached 15.5 mm. The tunneling process started to increase until Phase 12, where the settlement reached a maximum of 26.2 mm at the same location. This phase was verified with the Cairo metro [3], a maximum vertical displacement of about 20 mm. Also, this phase was the end of the tunneling process and the applied overburden pressure on the tunnel and can be represented in Fig. 2.

The next phase which is additional to the research this paper was verified with included the seismic load in the x-direction resulted in a maximum of 1.35 mm and minimum -0.55 mm lateral displacements at the tunnel portal crown. On the other hand, the last phase was applying the load in the z-direction, and the maximum vertical displacement was 28 mm. Figures 3 and 4 show the lateral and vertical displacements versus the portal's dynamic time, 2.5 m and 5 m away from the portal on the upper part of the tunnel shield during Phases 13 and 14, respectively. The negative and positive values represent the direction of the lateral displacements during seismic loading.